Acta Cryst C STRUCTURAL CHEMISTRY
ISSN 2053-2296

# Crystal structure, thermodynamic properties and detonation characterization of bis(5-amino-1,2,4-triazol-3-yl)methane

Hongya Li,[a] Biao Yan,[a]* Haixia Ma,[b] Zhiyong Sun,[c] Yajun Ma[a] and Zhifang Zhang[a]

[a]School of Chemistry and Chemical Engineering, Yulin University, Yulin 719000, Shaanxi, People's Republic of China, [b]School of Chemical Engineering, Northwest University, Xi'an 710069, Shaanxi, People's Republic of China, and [c]School of Energy Engineering, Yulin University, Yulin 719000, Shaanxi, People's Republic of China. *Correspondence e-mail: yanbiaoly@foxmail.com

Received 18 July 2019
Accepted 2 December 2019

Edited by B. D. Santarsiero, University of Illinois at Chicago, USA

**Keywords:** 1,2,4-triazole; BATZM; crystal structure; thermodynamics; detonation characterization; quantum chemistry.

**CCDC reference**: 1060496

**Supporting information**: this article has supporting information at journals.iucr.org/c

Bis(5-amino-1,2,4-triazol-3-yl)methane (BATZM, $C_5H_8N_8$) was synthesized and its crystal structure characterized by single-crystal X-ray diffraction; it belongs to the space group *Fdd*2 (orthorhombic) with $Z = 8$. The structure of BATZM can be described as a V-shaped molecule with reasonable chemical geometry and no disorder. The specific molar heat capacity ($C_{p,m}$) of BATZM was determined using the continuous $C_p$ mode of a microcalorimeter and theoretical calculations, and the $C_{p,m}$ value is 211.19 J K$^{-1}$ mol$^{-1}$ at 298.15 K. The relative deviations between the theoretical and experimental values of $C_{p,m}$, $H_T - H_{298.15K}$ and $S_T - S_{298.15K}$ of BATZM are almost equivalent at each temperature. The detonation velocity ($D$) and detonation pressure ($P$) of BATZM were estimated using the nitrogen equivalent equation according to the experimental density; BATZM has a higher detonation velocity (7954.87 ± 3.29 m s$^{-1}$) and detonation pressure (25.72 ± 0.03 GPa) than TNT.

## 1. Introduction

Triazole derivatives have been investigated as high-energy density materials (HEDMs) due to their high densities, high heats of formation and high thermal stability (Gao & Shreeve, 2011). The thermal stability of an energetic material is an important factor for its use and the desired decomposition temperature is above 473.15 K. For bis(5-amino-1,2,4-triazol-3-yl)methane (BATZM), the decomposition temperature is 566.15 K (Shreve & Charlesworth, 1956). It can be used as a precursor for the synthesis of bis-triazole-based energetic materials, such as bis(5-nitro-1,2,4-triazol-3-yl)methane (Bagal *et al.*, 1970), bis(5-nitro-2-nitroxymethyl-1,2,4-triazol-3-yl)nitromethane (Tselinskii *et al.*, 2009), bis(5-nitro-1,2,4-triazol-3-yl)-nitromethane (Tselinskii *et al.*, 2009), bis(5-nitro-1,2,4-triazol-3-yl)dinitromethane (Tselinskii *et al.*, 2009), bis(5-nitrimino-1,2,4-triazol-3-yl)methane (Dippold *et al.*, 2011) *etc*. In this article, BATZM was synthesized and its crystal structure is reported. The specific molar heat capacity ($C_{p,m}$) of BATZM was determined using the continuous $C_p$ mode of a micro-calorimeter and theoretical calculations. The detonation velocity ($D$) and pressure ($P$) of BATZM were also calculated to estimate its detonation properties.

## 2. Experimental

### 2.1. Synthesis and crystallization

The BATZM used in this work was prepared according to a modified literature procedure (Shreve & Charlesworth, 1956;

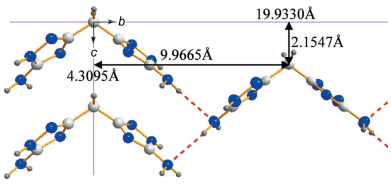


© 2020 International Union of Crystallography

Dippold *et al.*, 2011, 2012). Malonic acid (20.81 g, 0.2 mol) and aminoguanidine hydrochloride (44.22 g, 0.4 mol) were mixed with water (300 ml). The mixture was placed in a porcelain dish and evaporated to dryness on a steam bath. The white precipitate was dissolved in water (300 ml) and the pH was adjusted to 14 with sodium hydroxide. The reaction mixture was heated under reflux for 1 h and subsequently acidified with acetic acid to a pH value of 7. The white precipitate was collected by filtration and a colourless crystal of BATZM was obtained by recrystallization from water. Elemental analyses (C, H and N) were performed on an Elemental Analytical Instrument (PE-2400, PerkinElmer, USA). Analysis calculated (%) for $C_5H_8N_8$: C 33.33, H 4.48, N 62.19; found: C 33.45, H 4.40, N 62.05.

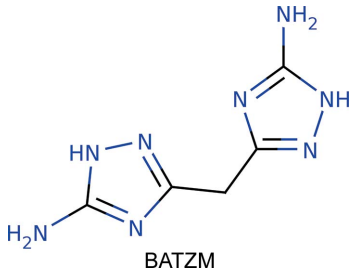

BATZM

### 2.2. Refinement

Crystal data, data collection and structure refinement details are summarized in Table 1. All H atoms were originally found in difference maps, but were treated differently in the refinement, with N—H distances restrained to 0.85 (1) Å, and with $U_{iso}$(H) = 1.2$U_{eq}$(N), while C—H distances were restrained to 0.99 Å, with $U_{iso}$(H) = 1.2$U_{eq}$(C) for methylene H atoms.

**Table 1**
Experimental details.

| | |
|---|---|
| Crystal data | |
| Chemical formula | $C_5H_8N_8$ |
| $M_r$ | 180.19 |
| Crystal system, space group | Orthorhombic, *Fdd*2 |
| Temperature (K) | 296 |
| *a*, *b*, *c* (Å) | 18.632 (3), 19.933 (3), 4.3095 (6) |
| *V* (Å$^3$) | 1600.6 (4) |
| *Z* | 8 |
| Radiation type | Mo *Kα* |
| $\mu$ (mm$^{-1}$) | 0.11 |
| Crystal size (mm) | 0.38 × 0.28 × 0.14 |
| Data collection | |
| Diffractometer | Bruker APEXII CCD |
| Absorption correction | Multi-scan (*SADABS*; Bruker, 2009) |
| $T_{min}$, $T_{max}$ | 0.960, 0.985 |
| No. of measured, independent and observed [$I > 2\sigma(I)$] reflections | 1858, 816, 757 |
| $R_{int}$ | 0.016 |
| (sin $\theta/\lambda)_{max}$ (Å$^{-1}$) | 0.661 |
| Refinement | |
| $R[F^2 > 2\sigma(F^2)]$, $wR(F^2)$, *S* | 0.028, 0.068, 1.07 |
| No. of reflections | 816 |
| No. of parameters | 73 |
| No. of restraints | 5 |
| H-atom treatment | H atoms treated by a mixture of independent and constrained refinement |
| $\Delta\rho_{max}$, $\Delta\rho_{min}$ (e Å$^{-3}$) | 0.12, −0.13 |
| Absolute structure | Flack *x* determined using 253 quotients $[(I^+) - (I^-)]/[(I^+) + (I^-)]$ (Parsons *et al.*, 2013) |
| Absolute structure parameter | 1.0 (10) |

Computer programs: *APEX2* (Bruker, 2009), *SAINT* (Bruker, 2009), *SHELXS97* (Sheldrick, 2008), *SHELXL2018* (Sheldrick, 2015) and *SHELXTL* (Sheldrick, 2008).

### 2.3. Heat capacity determination

The $C_{p,m}$ of BATZM was determined using a continuous $C_p$ mode from 283.15 to 353.15 K at a heating rate of 0.15 K min$^{-1}$ on a Micro-DSCIII (Setaram, France) instrument with a sample mass of 280.30 mg at a pressure of 101.3 kPa. The microcalorimeter was calibrated with $\alpha$-$Al_2O_3$ (calcined), its mathematical expression was $C_p$/(J K$^{-1}$ mol$^{-1}$) = 18.82369 + 2.033349 × 10$^{-1}$ ($T$/K) from 283.15 to 353.15 K, and the recommended equation is $C_p$/(J K$^{-1}$ mol$^{-1}$) = −1.32506 × 10$^8$ ($T$/K)$^{-3}$ + 4.54238 × 10$^6$ ($T$/K)$^{-2}$ − 5.475599 × 10$^4$ ($T$/K)$^{-1}$ + 2.574076 × 10$^2$ − 1.715032 × 10$^{-1}$ ($T$/K) + 1.2897189 × 10$^{-4}$ ($T$/K)$^2$ − 4.60768 × 10$^{-8}$ ($T$/K)$^3$ + 6.31755 × 10$^{-12}$ ($T$/K)$^4$ from 283.15 to 353.15 K (Ditmars *et al.*, 1982) (Fig. 1). The differences between the experimental and recommended values range from −0.50 to 1.59 J K$^{-1}$ mol$^{-1}$ over the temperature range from 283.15 to 353.15 K, the standard uncertainty is ±0.63 J K$^{-1}$ mol$^{-1}$ and the relative standard uncertainty is ±0.75%.

### 2.4. Quantum chemical calculations

The single-crystal structural data for BATZM were used in the theoretical calculations. The density functional theory (DFT) calculations were performed with the program package *DMol*$^3$ in *Materials Studio* (Version 8.0) of Accelrys Inc. on a personal computer (Delley, 1990, 2000). The generalized gradient approximation (GGA) with the RPBE functional (Hammer *et al.*, 1999) and double-numerical quality basis set with polarization functions (DNP) were used for all the atoms, the size of DNP being comparable to Gaussian 6-31G**. A thermal smearing of 2.0 × 10$^{-3}$ Hartree (Ha, 1 Ha = 27.2114 eV) and a real-space cut-off of 0.40 nm were adopted. For the numerical integration, the fine quality mesh size of the program was used. A 3 × 3 × 3 *k*-point sampling was applied in geometry optimization (Baker *et al.*, 1996; Andzelm *et al.*, 2001; Delley, 1996; Auckenthaler *et al.*, 2011). The convergences of energy, gradient and maximal displacement were set as 10$^{-5}$ Ha, 2.0 × 10$^{-1}$ Ha Å$^{-1}$ and 5.0 × 10$^{-3}$ Å, respectively. In addition, the frequency analysis (Baker *et al.*, 1996; Andzelm *et al.*, 2001; Delley, 1996) was performed to check if the stationary point was a potential minimum and to obtain the thermodynamic properties at different temperatures under atmospheric pressure.

## 3. Results and discussion

### 3.1. Crystal structure

Single-crystal analysis shows that BATZM crystallizes in the orthorhombic space group *Fdd*2 with $Z$ = 8. The molecule is

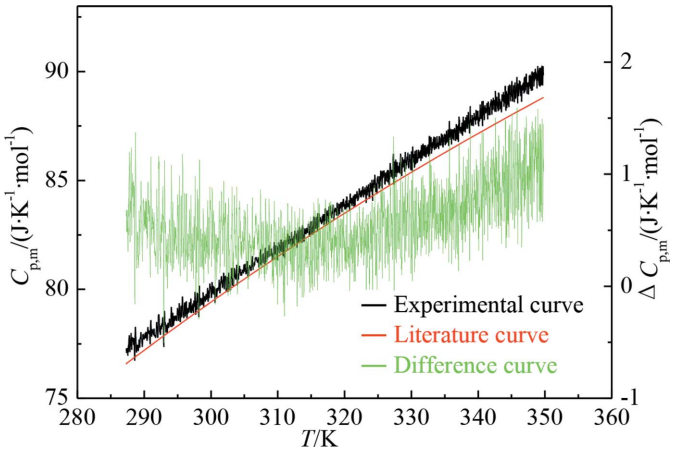


**Figure 1**
Experimental/literature/difference curves of the $C_{p,m}$ of $\alpha$-$Al_2O_3$.

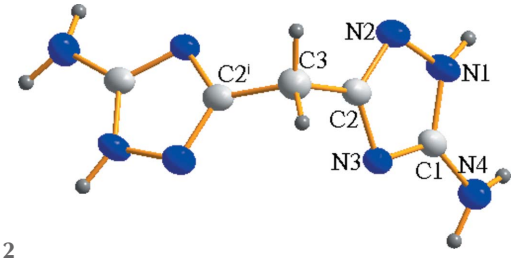


**Figure 2**
The molecular structure of BATZM. [Symmetry code: (i) $-x$, $-y$, $z$.]

characterized by two structural motifs: (i) internal symmetry and (ii) tight packing and extensive hydrogen bonding (Table 2). Fig. 2 illustrates that the molecule has an internal twofold axis which passes through atom C3 and is parallel to the *c* axis, with reasonable chemical geometry and no disorder. Fig. 3 illustrates that each BATZM molecule is cross-connected with four BATZM molecules through a hydrogen bond (N4—H4*B*···N4$^{iii}$; Table 2) to form a 2D network. Viewed along the *c*-axis direction, the distance between adjacent BATZM molecules is the same as the *c* unit-cell length. One BATZM molecule moves half a *b* unit-cell length along the *b* axis and half a *c* unit-cell length along the *c* axis to generate another BATZM molecule. The N1—H1···N3$^{ii}$ and N4$^{iii}$—H4*A*···N2$^{v}$ hydrogen bonds [Table 2; additionally symmetry code: (v) $-x-\frac{1}{4}, y+\frac{1}{4}, z-\frac{1}{4}$] are connected with the adjacent two-dimensional (2D) substructure to form a three-dimensional (3D) network (Fig. 4). The distance between

**Table 2**
Hydrogen-bond geometry (Å, °).

| *D*—H···*A* | *D*—H | H···*A* | *D*···*A* | *D*—H···*A* |
|---|---|---|---|---|
| N1—H1···N3$^{ii}$ | 0.85 (1) | 1.98 (1) | 2.782 (2) | 157 (2) |
| N4—H4*B*···N4$^{iii}$ | 0.87 (1) | 2.52 (2) | 3.204 (2) | 136 (2) |
| N4—H4*A*···N2$^{iv}$ | 0.86 (1) | 2.22 (1) | 3.082 (2) | 174 (2) |

Symmetry codes: (ii) $x+\frac{1}{4}, -y+\frac{1}{4}, z+\frac{1}{4}$; (iii) $-x, -y+\frac{1}{2}, z+\frac{1}{2}$; (iv) $x-\frac{1}{4}, -y+\frac{1}{4}, z+\frac{3}{4}$.

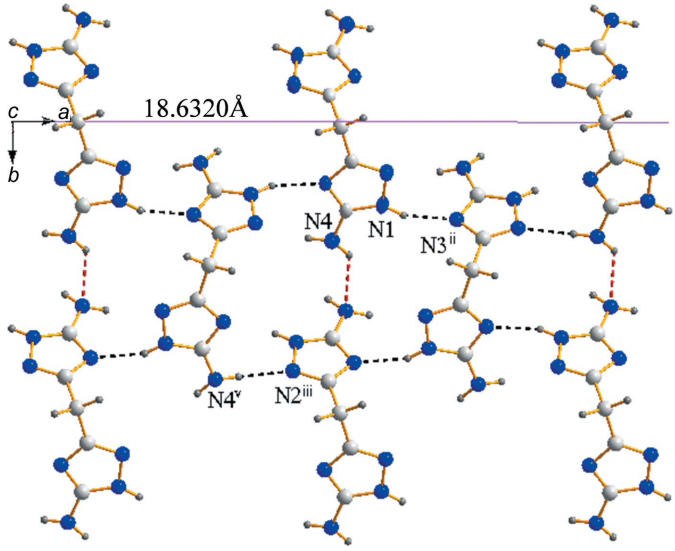


**Figure 4**
The 3D structure of BATZM. [Symmetry codes: (ii) $x+\frac{1}{4}, -y+\frac{1}{4}, z+\frac{1}{4}$; (iii) $-x, -y+\frac{1}{2}, z+\frac{1}{2}$; (v) $-x-\frac{1}{4}, y+\frac{1}{4}, z-\frac{1}{4}$.]

adjacent 2D structures is quarter of the *a* unit-cell length along the *a*-axis direction. The packing diagram of BATZM, viewed down the *c* axis, is shown in Fig. 5.

### 3.2. Specific heat capacity

The $C_{p,m}$ of BATZM was measured using the continuous $C_p$ mode of a Micro-DSCIII apparatus and is shown in Fig. 6. It was found that the $C_{p,m}$ of BATZM is modelled by a good linear relationship between temperatures from 287.29 to 349.78 K and the $C_{p,m}$ equation can be defined as:

$$C_{p,m}(\text{BATZM})/(\text{J K}^{-1}\ \text{mol}^{-1}) = 1.64295 \times 10 + 6.53247 \times 10^{-1}(T/\text{K}). \quad (1)$$

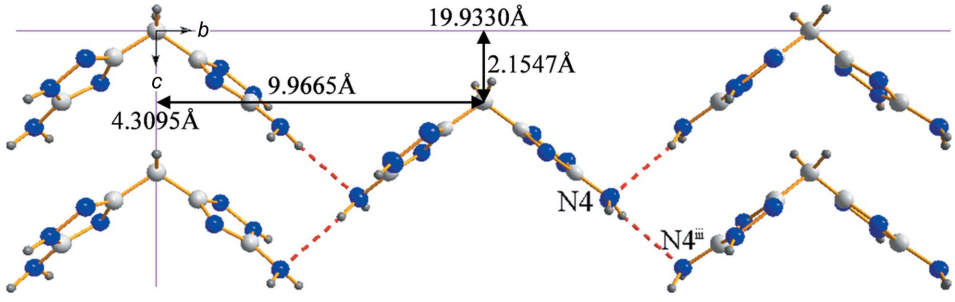


**Figure 3**
The 2D structure of BATZM. [Symmetry code: (iii) $-x, -y+\frac{1}{2}, z+\frac{1}{2}$.]

**Table 3**
Thermodynamic properties of BATZM at a pressure of 101.3 kPa.

| $T$ (K) | $C_{p,m}$ (J K$^{-1}$ mol$^{-1}$) | | RD | $H_T - H_{298.15K}$ (kJ mol$^{-1}$) | | RD | $S_T - S_{298.15K}$ (J K$^{-1}$ mol$^{-1}$) | | RD |
|---|---|---|---|---|---|---|---|---|---|
| | Exp | Calc | | Exp | Calc | | Exp | Calc | |
| 288.15 | 204.66 | 182.58 | 10.79 | −2.08 | −1.85 | 10.83 | −7.09 | −6.33 | 10.82 |
| 293.15 | 207.93 | 185.44 | 10.81 | −1.05 | −0.93 | 10.85 | −3.54 | −3.16 | 10.83 |
| 298.15 | 211.19 | 188.29 | 10.84 | – | – | – | – | – | – |
| 303.15 | 214.46 | 191.13 | 10.88 | 1.06 | 0.95 | 10.88 | 3.54 | 3.15 | 10.86 |
| 308.15 | 217.73 | 193.96 | 10.92 | 2.14 | 1.91 | 10.90 | 7.07 | 6.30 | 10.88 |
| 313.15 | 220.99 | 196.77 | 10.96 | 3.24 | 2.89 | 10.92 | 10.61 | 9.45 | 10.90 |
| 318.15 | 224.26 | 199.58 | 11.01 | 4.35 | 3.88 | 10.93 | 14.13 | 12.59 | 10.92 |
| 323.15 | 227.53 | 202.37 | 11.06 | 5.48 | 4.88 | 10.95 | 17.65 | 15.72 | 10.94 |
| 328.15 | 230.79 | 205.15 | 11.11 | 6.63 | 5.90 | 10.96 | 21.17 | 18.85 | 10.96 |
| 333.15 | 234.06 | 207.92 | 11.17 | 7.79 | 6.94 | 10.98 | 24.69 | 21.97 | 10.99 |
| 338.15 | 237.32 | 210.67 | 11.23 | 8.97 | 7.98 | 10.99 | 28.20 | 25.09 | 11.01 |
| 343.15 | 240.59 | 213.42 | 11.29 | 10.17 | 9.05 | 11.01 | 31.71 | 28.21 | 11.04 |
| 348.15 | 243.86 | 216.15 | 11.36 | 11.38 | 10.12 | 11.02 | 35.21 | 31.31 | 11.07 |

Notes: Exp is the result of an experimental determination; Calc is the result of a theoretical calculation; RD = $10^2(X_{Exp} - X_{Calc})/X_{Exp}$; $H_T - H_{298.15K}$ is the enthalpy change when taking 298.15 K as the benchmark; $S_T - S_{298.15K}$ is the entropy change when taking 298.15 K as the benchmark.

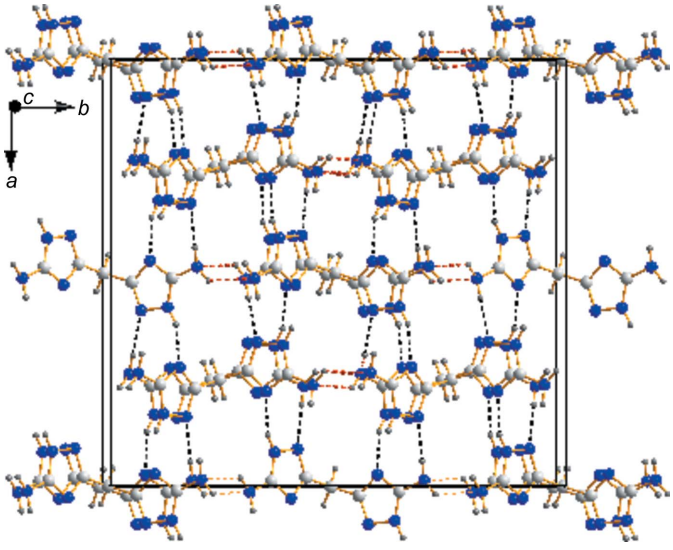


**Figure 5**
Packing diagram of BATZM, viewed down the *c* axis.

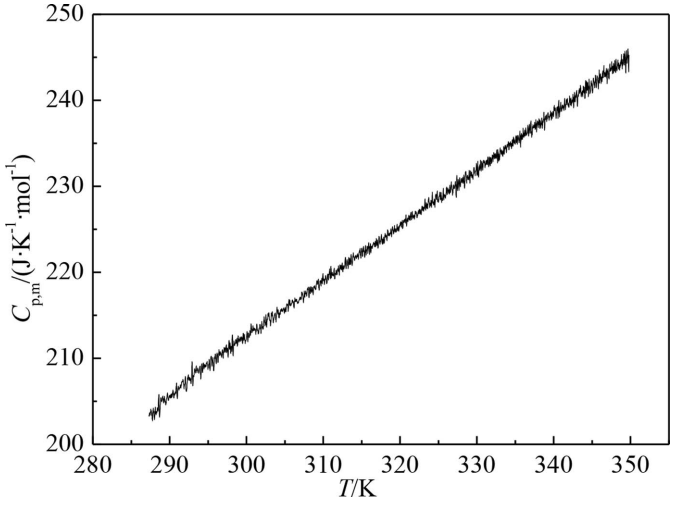


**Figure 6**
Determination of the continuous $C_{p,m}$ of BATZM.

The correlation coefficients of the fitting ($R^2$) and the standard deviation (SD) results are 0.99868 and 0.42937, respectively. The $C_{p,m}$ value of BATZM is 211.19 J K$^{-1}$ mol$^{-1}$ at 298.15 K.

Table 3 shows a comparison between the $C_{p,m}$ values of BATZM obtained by theoretical calculation (Calc) and experimental determination (Exp), and their relative deviations (RD) at different temperatures. The theoretical calculation results are all less than the experimental determination results, and the relative deviations vary from 10.77 to 11.43%. These results are similar to those observed for *N*-benzoyl-3,3-dinitroazetidine (Yan *et al.*, 2012), *N*-(2,4-dinitrophenyl)-3,3-dinitroazetidine (Yan *et al.*, 2014), *N*-acetyl-3,3-dinitroazetidine (Li *et al.*, 2015), hexaconazole (Yan *et al.*, 2016*a*), myclobutanil (Yan *et al.*, 2016*a*), diniconazole (Yan *et al.*, 2016*c*), 3,3-dinitroazetidinium perchlorate (Yan *et al.*, 2016*b*) and 3,3-dinitroazetidinium chloride (Yan *et al.*, 2016*b*).

### 3.3. Thermodynamic properties

The enthalpy change and entropy change of BATZM were calculated using equations (2) and (3) from 287.29 to 349.78 K taking 298.15 K as the benchmark, and the results are listed in Table 3. The absolute values of the theoretical calculations of BATZM are all lower than those of the experimental determination, and the relative deviations of $H_T - H_{298.15K}$ and $S_T - S_{298.15K}$ of BATZM are almost equivalent at each temperature, and the relative deviations (10.80–11.09%) vary only slightly.

$$H_T - H_{2.9815K}/(\text{J mol}^{-1}) = \int_{2.9815K}^{T} C_{p,m}\mathrm{d}T/(\text{J mol}^{-1}) \quad (2)$$

$$S_T - S_{2.9815K}/(\text{J K}^{-1}\text{ mol}^{-1}) = \int_{298.15K}^{T} C_{p,m}\cdot T^{-1}\mathrm{d}T/(\text{J K}^{-1}\text{mol}^{-1}) \quad (3)$$

### 3.4. Characterization of detonation velocity and pressure

Detonation velocity ($D$) and pressure ($P$) are the most important targets for scaling the detonation characteristics of

Table 4
Nitrogen equivalents of different detonation products.

| Detonation product | C | $H_2$ | $N_2$ | CO | $CO_2$ |
|---|---|---|---|---|---|
| Nitrogen equivalent index | 0.15 | 0.29 | 1 | 0.78 | 1.35 |

energetic materials. The $D$ and $P$ values of an explosive material can be predicted by the nitrogen equivalent equation shown as equations (4) to (6) (Guo & Zhang, 1983).

$$\sum N = 100 \sum x_i N_i / M \tag{4}$$

$$D = (690 + 1160\rho) \sum N \tag{5}$$

$$P = 1.092\left(\rho \sum N\right)^2 - 0.574. \tag{6}$$

Where $\Sigma N$ is the nitrogen equivalent of the detonation products, $x_i$ is the mole number of a certain detonation product produced by a mole explosive, $N_i$ is the nitrogen equivalent index of a certain detonation product, $M$ is the molecular weight of an explosive (g mol$^{-1}$) and $\rho$ is the density of an explosive (g cm$^{-3}$).

The detonation products produced by explosives together with their nitrogen equivalent indices are listed in Table 4. According to the order $H_2O \rightarrow CO \rightarrow CO_2$ in forming detonation products, the detonation products of BATZM are calculated as follows:

$$C_5H_8N_8 = (5)C + (4)H_2 + (4)N_2$$

According to equation (4), in which $M$ = 180.19 g mol$^{-1}$ and $\rho$ = 1.496 ± 0.001 g cm$^{-3}$, the total nitrogen equivalents of BATZM are obtained through the nitrogen equivalent indices of the detonation products in Table 4:

$$\sum N = 100 \times (5 \times 0.15 + 4 \times 0.29 + 4 \times 1)/180.19 = 3.280.$$

The $D$ and $P$ values can be obtained according to equations (5) and (6), *viz.* 7954.87 ± 3.29 m s$^{-1}$ and 25.72 ± 0.03 GPa, respectively, which are greater than those of trinitrotoluene (TNT; 6881 m s$^{-1}$ and 19.5 GPa; Wang *et al.*, 2010) and less than those of 1,3,5-triamino-2,4,6-trinitrobenzene (TATB; 8114 m s$^{-1}$ and 31.2 GPa; Wang *et al.*, 2010).

## 4. Conclusions

The structure of BATZM is found to crystallize in the space group *Fdd2* (orthorhombic) with a highly dense 2D and 3D network structure. The $C_{p,m}$ equation of BATZM is $C_{p,m}$/(J K$^{-1}$ mol$^{-1}$) = 1.64295 × 10 + 6.53247 × 10$^{-1}$ ($T$/K) and the $C_{p,m}$ is 211.19 J K$^{-1}$ mol$^{-1}$ at 298.15 K. The relative deviations of $C_{p,m}$, $H_T - H_{298.15K}$ and $S_T - S_{298.15K}$ of BATZM are almost equivalent at each temperature and their relative deviations change little. The $D$ and $P$ values of BATZM are 7954.87 ± 3.29 m s$^{-1}$ and 25.72 ± 0.03 GPa, respectively, which are greater than those of TNT and less than those of TATB.

## Funding information

Funding for this research was provided by: National Natural Science Foundation of China (grant Nos. 21673179, 21663033 and 21763030); Provincial Natural Science Foundation of Shaanxi (grant No. 2019SF-271); Yulin City Industry-University-Research Cooperation Project (grant No. 2016CXY-05-01); Startup Foundation for Advanced Talents of Yulin University (award No. 16GK10).

## References

Andzelm, J., King-Smith, R. D. & Fitzgerald, G. (2001). *Chem. Phys. Lett.* **335**, 321–326.
Auckenthaler, T., Blum, V., Bungartz, H. J., Huckle, T., Johanni, R., Krämer, L., Lang, B., Lederer, H. & Willems, P. R. (2011). *Parallel Comput.* **37**, 783–794.
Bagal, L. I., Pevzner, M. S., Frolov, A. N. & Sheludyakova, N. I. (1970). *Chem. Heterocycl. Compd.* **6**, 240–244.
Baker, J., Kessi, A. & Delley, B. (1996). *J. Chem. Phys.* **105**, 192–212.
Bruker (2009). *APEX2*, *SAINT* and *SADABS*. Bruker AXS Inc., Madison, Wisconsin, USA.
Delley, B. (1990). *J. Chem. Phys.* **92**, 508–517.
Delley, B. (1996). *J. Phys. Chem.* **100**, 6107–6110.
Delley, B. (2000). *J. Chem. Phys.* **113**, 7756–7764.
Dippold, A. A., Feller, M. & Klapötke, T. M. (2011). *Cent. Eur. J. Energ. Mat.* **8**, 261–278.
Dippold, A. A., Klapötke, T. M. & Winter, N. (2012). *Eur. J. Inorg. Chem.* **2012**, 3474–3484.
Ditmars, D. A., Ishihara, S., Chang, S.-S., Bernstein, G. & West, E. D. (1982). *J. Res. Natl. Bur. Stan.* **87**, 159–163.
Gao, H.-X. & Shreeve, J. M. (2011). *Chem. Rev.* **111**, 7377–7436.
Guo, Y.-X. & Zhang, H.-S. (1983). *Explos. Shock Waves*, **3**, 5623–5629.
Hammer, B., Hansen, L. B. & Nørskov, J. K. (1999). *Phys. Rev. B*, **59**, 7413–7421.
Li, H.-Y., Yan, B., Bai, K.-Q., Liu, H., Ma, H.-X., Song, J.-R. & Yan, L. (2015). *J. Chem. Thermodyn.* **91**, 240–244.
Parsons, S., Flack, H. D. & Wagner, T. (2013). *Acta Cryst.* B**69**, 249–259.
Sheldrick, G. M. (2008). *Acta Cryst.* A**64**, 112–122.
Sheldrick, G. M. (2015). *Acta Cryst.* C**71**, 3–8.
Shreve, R. N. & Charlesworth, R. K. (1956). US Patent 2744116.
Tselinskii, I. V., Tolstyakov, V. V., Putis, S. M. & Mel'nikova, S. F. (2009). *Russ. Chem. Bull.* **58**, 2356–2361.
Wang, R.-H., Xu, H.-Y., Guo, Y., Sa, R.-J. & Shreeve, J. M. (2010). *J. Am. Chem. Soc.* **132**, 11904–11905.
Yan, B., Li, H.-Y., Gao, J., Wang, A.-M., Ren, G.-Y., Li, Y.-J. & Ma, H.-X. (2016*a*). *J. Chem. Thermodyn.* **99**, 82–85.
Yan, B., Li, H.-Y., Guan, Y.-L., Ma, H.-X., Song, J.-R. & Zhao, F.-Q. (2016*c*). *J. Chem. Thermodyn.* **103**, 206–211.
Yan, B., Li, H.-Y., Zhao, N.-N., Ma, H.-X., Song, J.-R., Zhao, F.-Q. & Hu, R.-Z. (2014). *J. Chem. Thermodyn.* **69**, 152–156.
Yan, B., Li, J., Li, H.-Y., Gao, J., Wang, A.-M., Ren, G.-Y. & Ma, H.-X. (2016*b*). *J. Chem. Thermodyn.* **101**, 44–48.
Yan, B., Zhao, N.-N., Mai, T., Xu, K.-Z., Ma, H.-X. & Song, J.-R. (2012). *Russ. J. Phys. Chem.* A**86**, 1962–1968.

# supporting information

*Acta Cryst.* (2020). C**76**, 64-68 [https://doi.org/10.1107/S2053229619016231]

# Crystal structure, thermodynamic properties and detonation characterization of bis(5-amino-1,2,4-triazol-3-yl)methane

**Hongya Li, Biao Yan, Haixia Ma, Zhiyong Sun, Yajun Ma and Zhifang Zhang**

## Computing details

Data collection: *APEX2* (Bruker, 2009); cell refinement: *SAINT* (Bruker, 2009); data reduction: *SAINT* (Bruker, 2009); program(s) used to solve structure: *SHELXS97* (Sheldrick, 2008); program(s) used to refine structure: *SHELXL2018* (Sheldrick, 2015); molecular graphics: *SHELXTL* (Sheldrick, 2008); software used to prepare material for publication: *SHELXTL* (Sheldrick, 2008).

## Bis(5-amino-1,2,4-triazol-3-yl)methane

### *Crystal data*

$C_5H_8N_8$
$M_r$ = 180.19
Orthorhombic, *Fdd*2
*a* = 18.632 (3) Å
*b* = 19.933 (3) Å
*c* = 4.3095 (6) Å
*V* = 1600.6 (4) Å$^3$
*Z* = 8
*F*(000) = 752
$D_x$ = 1.496 Mg m$^{-3}$
Mo *Kα* radiation, $\lambda$ = 0.71073 Å
Cell parameters from 918 reflections
$\theta$ = 3.0–25.9°
$\mu$ = 0.11 mm$^{-1}$
*T* = 296 K
Acicular, colourless
0.38 × 0.28 × 0.14 mm

### *Data collection*

Bruker APEXII CCD diffractometer
$\varphi$ and $\omega$ scans
Absorption correction: multi-scan (SADABS; Bruker, 2009)
$T_{min}$ = 0.960, $T_{max}$ = 0.985
1858 measured reflections
816 independent reflections
757 reflections with $I > 2\sigma(I)$
$R_{int}$ = 0.016
$\theta_{max}$ = 28.0°, $\theta_{min}$ = 3.0°
*h* = −24→23
*k* = −9→24
*l* = −5→4

### *Refinement*

Refinement on $F^2$
Least-squares matrix: full
$R[F^2 > 2\sigma(F^2)]$ = 0.028
$wR(F^2)$ = 0.068
*S* = 1.07
816 reflections
73 parameters
5 restraints
Primary atom site location: structure-invariant direct methods
Secondary atom site location: difference Fourier map
Hydrogen site location: mixed
H atoms treated by a mixture of independent and constrained refinement
$w = 1/[\sigma^2(F_o^2) + (0.0322P)^2 + 0.6778P]$ where $P = (F_o^2 + 2F_c^2)/3$
$(\Delta/\sigma)_{max} < 0.001$
$\Delta\rho_{max}$ = 0.12 e Å$^{-3}$
$\Delta\rho_{min}$ = −0.13 e Å$^{-3}$
Extinction correction: SHELXL2018 (Sheldrick, 2015), $Fc^*=kFc[1+0.001xFc^2\lambda^3/\sin(2\theta)]^{-1/4}$
Extinction coefficient: 0.0044 (7)

Absolute structure: Flack *x* determined using 253 quotients [(I+)-(I-)]/[(I+)+(I-)] (Parsons *et al.*, 2013)
Absolute structure parameter: 1.0 (10)

*Special details*

**Geometry**. All esds (except the esd in the dihedral angle between two l.s. planes) are estimated using the full covariance matrix. The cell esds are taken into account individually in the estimation of esds in distances, angles and torsion angles; correlations between esds in cell parameters are only used when they are defined by crystal symmetry. An approximate (isotropic) treatment of cell esds is used for estimating esds involving l.s. planes.

*Fractional atomic coordinates and isotropic or equivalent isotropic displacement parameters (Å²)*

| | *x* | *y* | *z* | $U_{iso}$*/$U_{eq}$ |
|---|---|---|---|---|
| N2 | 0.08768 (7) | 0.07813 (8) | −0.1174 (4) | 0.0339 (4) |
| C3 | 0.000000 | 0.000000 | −0.3477 (7) | 0.0320 (6) |
| C1 | 0.01192 (9) | 0.14092 (9) | 0.1546 (4) | 0.0266 (4) |
| N3 | −0.02808 (7) | 0.09508 (7) | 0.0117 (4) | 0.0268 (4) |
| C2 | 0.02091 (9) | 0.05860 (8) | −0.1521 (4) | 0.0261 (4) |
| N1 | 0.08068 (7) | 0.13222 (8) | 0.0808 (4) | 0.0341 (4) |
| N4 | −0.01377 (9) | 0.19194 (8) | 0.3320 (4) | 0.0358 (5) |
| H3 | 0.0419 (9) | −0.0126 (10) | −0.478 (5) | 0.043* |
| H4A | −0.0565 (7) | 0.1859 (10) | 0.403 (6) | 0.043* |
| H4B | 0.0172 (9) | 0.2130 (10) | 0.448 (5) | 0.043* |
| H1 | 0.1188 (8) | 0.1486 (9) | 0.160 (5) | 0.043* |

*Atomic displacement parameters (Å²)*

| | $U^{11}$ | $U^{22}$ | $U^{33}$ | $U^{12}$ | $U^{13}$ | $U^{23}$ |
|---|---|---|---|---|---|---|
| N2 | 0.0245 (7) | 0.0391 (8) | 0.0380 (10) | −0.0006 (6) | 0.0033 (8) | −0.0040 (8) |
| C3 | 0.0329 (13) | 0.0359 (14) | 0.0271 (16) | −0.0005 (11) | 0.000 | 0.000 |
| C1 | 0.0222 (8) | 0.0302 (9) | 0.0272 (11) | −0.0002 (7) | −0.0004 (8) | 0.0060 (8) |
| N3 | 0.0203 (7) | 0.0297 (8) | 0.0303 (9) | −0.0003 (6) | −0.0006 (7) | 0.0022 (6) |
| C2 | 0.0233 (8) | 0.0304 (9) | 0.0246 (10) | 0.0004 (7) | 0.0011 (8) | 0.0056 (8) |
| N1 | 0.0199 (7) | 0.0411 (9) | 0.0412 (10) | −0.0047 (7) | −0.0016 (7) | −0.0058 (8) |
| N4 | 0.0311 (8) | 0.0363 (9) | 0.0398 (12) | −0.0032 (7) | 0.0040 (9) | −0.0069 (8) |

*Geometric parameters (Å, º)*

| | | | |
|---|---|---|---|
| N2—C2 | 1.312 (2) | C1—N1 | 1.332 (2) |
| N2—N1 | 1.382 (2) | C1—N4 | 1.359 (2) |
| C3—C2 | 1.492 (2) | N3—C2 | 1.364 (2) |
| C3—C2$^{i}$ | 1.492 (2) | N1—H1 | 0.853 (12) |
| C3—H3 | 0.993 (16) | N4—H4A | 0.861 (12) |
| C3—H3$^{i}$ | 0.993 (16) | N4—H4B | 0.871 (12) |
| C1—N3 | 1.330 (2) | | |
| | | | |
| C2—N2—N1 | 102.28 (14) | C1—N3—C2 | 103.35 (14) |
| C2—C3—C2$^{i}$ | 111.2 (2) | N2—C2—N3 | 114.66 (16) |

| | | | |
|---|---|---|---|
| C2—C3—H3 | 108.1 (12) | N2—C2—C3 | 122.98 (14) |
| C2$^{i}$—C3—H3 | 109.1 (12) | N3—C2—C3 | 122.34 (14) |
| C2—C3—H3$^{i}$ | 109.1 (12) | C1—N1—N2 | 109.88 (15) |
| C2$^{i}$—C3—H3$^{i}$ | 108.1 (12) | C1—N1—H1 | 130.9 (15) |
| H3—C3—H3$^{i}$ | 111 (3) | N2—N1—H1 | 117.9 (14) |
| N3—C1—N1 | 109.83 (16) | C1—N4—H4A | 114.9 (15) |
| N3—C1—N4 | 125.24 (15) | C1—N4—H4B | 116.7 (14) |
| N1—C1—N4 | 124.79 (16) | H4A—N4—H4B | 118 (2) |
| | | | |
| N1—C1—N3—C2 | −0.1 (2) | C2$^{i}$—C3—C2—N2 | 106.21 (19) |
| N4—C1—N3—C2 | 175.64 (18) | C2$^{i}$—C3—C2—N3 | −72.01 (15) |
| N1—N2—C2—N3 | −1.0 (2) | N3—C1—N1—N2 | −0.5 (2) |
| N1—N2—C2—C3 | −179.38 (17) | N4—C1—N1—N2 | −176.29 (17) |
| C1—N3—C2—N2 | 0.8 (2) | C2—N2—N1—C1 | 0.92 (19) |
| C1—N3—C2—C3 | 179.12 (18) | | |

Symmetry code: (i) −*x*, −*y*, *z*.

*Hydrogen-bond geometry (Å, º)*

| *D*—H···*A* | *D*—H | H···*A* | *D*···*A* | *D*—H···*A* |
|---|---|---|---|---|
| N1—H1···N3$^{ii}$ | 0.85 (1) | 1.98 (1) | 2.782 (2) | 157 (2) |
| N4—H4*B*···N4$^{iii}$ | 0.87 (1) | 2.52 (2) | 3.204 (2) | 136 (2) |
| N4—H4*A*···N2$^{iv}$ | 0.86 (1) | 2.22 (1) | 3.082 (2) | 174 (2) |

Symmetry codes: (ii) *x*+1/4, −*y*+1/4, *z*+1/4; (iii) −*x*, −*y*+1/2, *z*+1/2; (iv) *x*−1/4, −*y*+1/4, *z*+3/4.